***Supporting Information***

# Click-based porous ionic polymers with intercalated high-density metalloporphyrin for sustainable $CO_2$ transformation

Yaju Chen,[†,I] Rongchang Luo,*[,‡] Qinggang Ren,[§] Xiantai Zhou,[I] and Hongbing Ji*[,†,I]

[†] School of Chemistry, Guangdong University of Petrochemical Technology, Maoming 525000, China
[‡] School of Chemical Engineering and Light Industry, Guangdong University of Technology, Guangzhou 510006, China
[§] School of Materials Science and Engineering, Guangdong University of Petrochemical Technology, Maoming 525000, China
[I] Fine Chemical Industry Research Institute, School of Chemistry, Key Laboratory of Low-Carbon Chemistry & Energy Conservation of Guangdong Province, Sun Yat-sen University, Guangzhou 510275, China

* Corresponding authors: jihb@mail.sysu.edu.cn (Hongbing Ji), luorch@gdut.edu.cn (Rongchang Luo)

## 1. Characterization

Fourier transform infrared spectroscopy (FTIR) spectra of the samples were obtained under ambient conditions at a resolution of 4 $cm^{-1}$ in the wave number range of 4000-400 $cm^{-1}$ by using an EQUINOX 55 spectrometer. Elemental analyses for C, H, and N were detected on a Vario EL cube instrument. Inductively coupled plasma optical emission spectroscopy (ICP-OES) was performed on OPTIMA 8000DV (PerkinElmer). Thermogravimetry and differential thermogravimetric (TG-DTG) was carried out in a NETZSCH TG 209 F3 Tarsus instrument by heating samples from 40 °C to 850 °C at a heating rate of 10 °C·$min^{-1}$ under air atmosphere. Liquid $^{1}H$ and $^{13}C$ NMR data were collected on a Bruker Varian INOVA500NB or Bruker AVANCE 400 spectrometer using TMS as an internal standard. The experimental parameters were as follows: 5 s relaxation delay and 16 scans for $^{1}H$ NMR, and 1.55 s relaxation delay and 1800 scans for $^{13}H$ NMR. The Solid-state $^{13}C$ NMR spectrum was recorded on Bruker AVANCE 400 spectrometer. The experimental parameters were as follows: 2 s relaxation delay 2500 scans. Matrix-assisted laser desorption/ionization time-of-flight mass spectroscopy (MALDI-TOF/MS) was performed on a Bruker ultrafleXtreme MALDI TOF mass spectrometer using trans-2-[3-(4-tert-Butylphenyl)-2-methyl-2-propenylidene]malononitrile (DCTB) as matrix. The halogen content was measured by oxygen flask combustion and mercury nitrate titration technique. X-ray photoelectron spectroscopy (XPS) analysis was carried out on an ESCALAB 250 spectrometer. Field emission scanning electron microscopy (SEM) images were obtained by a FEI Quanta 400 FEG. Transmission electron microscopy (TEM) and EDX-mapping experiments were performed on JEM-2100F field emission electron microscope (JEOL, Japan) with an acceleration voltage of 200 kV, which incorporated a probe corrector and a super-X EDS system. The $N_2$ adsorption and desorption measurements were performed on a Micromeritic ASAP2020M analyzer at 77 K. Specific surface areas ($S_{BET}$) were calculated using Brunauer-Emmett-Teller (BET) methods and the pore size distributions were analyzed by using nonlocal density functional theory (NLDFT). The isosteric heats of adsorption ($Q_{st}$) for $CO_2$ were calculated from the Clausius–Clapeyron equation by using the $CO_2$ adsorption isotherms at 273 and 298 K. All samples were degassed at 130 °C for 10 h under vacuum before analysis. X-Ray diffraction patterns of the powder samples were obtained with a Bruker AXS D8 Advanced SWAX diffractometer by depositing powder on glass substrate, from $2\theta = 4.0°$ to 60° with 0.1° increment at 25 °C. Isotherms of carbon dioxide were collected from Micromeritic ASAP2020M at 273 K

and 298 K. Gas chromatographic (GC) analysis was performed on a GC2010 gas chromatograph (Shimadzu) equipped with a flame ionization detection and a capillary column (Rtx-5, 30 m × 0.32 mm × 0.25 μm) to determine the conversion (conversion = {[(total moles of epoxide) – (moles of residual alcohol)]/[total moles of alcohol]} × 100%) and yield (yield = {[moles of targeted product]/[total moles of epoxide]} × 100%).

## 2. Synthesis

*Synthesis of 5,10,15,20-tetra-(4-nitrophenyl)porphyrin (TNPP)*[1]. A solution of 4-nitrobenzaldehyde (11.0 g, 73 mmol) and acetic anhydride (12 mL, 127 mmol) in propionic acid (300 mL) was heated to 120 °C. The mixture of freshly distilled pyrrole (5.0 mL, 73 mmol) in propionic acid (100 mL) was added slowly, and the reaction solution was stirred at 140 °C for 2 h. Upon cooling, the mixture was refrigerated overnight, and then the resulted precipitate was collected by filtration and washed with methanol (5 × 100 mL) and deionized water (5 × 100 mL). Next, the obtained dark solid was dissolved in pyridine (80 mL) and refluxed for 1 h. After cooling down, the system was refrigerated overnight. The desired purple product (TNPP) was obtained by filtering, washing with the mixture of methanol/acetone and vacuum drying (yield, 21.2 %).

*Synthesis of 5,10,15,20-tetra-(4-aminophenyl)porphyrin (TAPP)*[2]. To a mixture of TNPP (1.8 g) in concentrated hydrochloric acid (75 mL), a solution of $SnCl_2$ (7.0 g, 29 mmol) in 20 mL of concentrated hydrochloric acid was dropwise added under $N_2$ atmosphere. After stirring at room temperature for 2.5 h, the reaction mixture was heated to 80 °C for 1 h, last chilled to 0 °C. Then the mixture was neutralized with ammonium hydroxide at 0 °C, and the green solid was obtained via vacuum filtration followed by dispersion in sodium hydroxide aqueous (200 mL, 5 %). Finally, the raw product was purified by Soxhlet extraction with chloroform to give purple TAPP (yield, 78 %). $^1$H NMR (500 MHz, $CDCl_3$, 25 °C) δ 8.90 (s, 8H, pyrrole ring), 7.991 (d, $J$ =8.2 Hz, 8H, ArH), 7.07 (d, $J$ = 8.2 Hz, 8H, ArH), 4.03 (s, 8H, $NH_2$), -2.71 (s, 2H, pyrrole NH)

*Synthesis of 5,10,15,20-tetrakis(4-aminophenyl)porphinato]cobalt(III) chloride ($Co^{III}$-TAPP).* Following a modified procedure from reference [3]*:* Briefly, to a mixture of TAPP (0.3 mmol, 200 mg) and NaOAc (1.3 mmol, 108 mg) in a 45 mL of DMF/chlorobenzene (2/3, v/v) , $Co(OAc)_2{\cdot}4H_2O$ (0.6 mmol, 149 mg) was added under cold condition. After equipping with a Soxhelt apparatus with a paper thimble containing $K_2CO_3$ (8.0 mmol, 1.1 g), the reaction mixture was stirred under nitrogen at reflux for 24 h. After cooling down to room temperature, the mixture was evaporated under reduced pressure. Obtained solid was suspended in $CHCl_3$ (100 mL) and the solvent was removed through vacuum filtration. The crude product was then washed thoroughly with water (3 × 20 mL), saturate $NaHCO_3$ solution (1 × 20 mL), and then water again (3 × 20 mL).

The resulting dark purple powder ($Co^{II}$-TAPP, 76%) was dried under high vacuum at 80 °C for 12 h. MALDI-TOF MS: m/z calcd for $C_{44}H_{32}CoN_8$, 731.21; found, 731.18. UV-Vis (in DMF): 450, 550, 600 nm.

Finally, to a solution of $Co^{II}$-TAPP (0.2 mmol, 146 mg) in DMF (50 mL), HCl (1.5 mmol, 0.15 mL) was added under cold condition. After stirring for 12 h under air atmosphere, the solvent was removed under vacuum. The residue was washed with saturate $NaHCO_3$ solution (1 × 20 mL) and water again (3 × 20 mL). The resulting dark purple powder ($Co^{III}$-TAPP, 96%) was dried under vacuum at 80 °C before being subjected to the following synthesis.

## 3. Elemental Analysis and ICP Analysis

**Table S1** Elemental analysis and ICP analysis of catalysts.

| Sample | CHN Elemental Analysis (wt%) | | | halogen content (mmol $g^{-1}$) | Co content (mmol $g^{-1}$) |
|---|---|---|---|---|---|
| | C | H | N | | |
| imine-TPP-POP | 80.25 (80.20)[a] | 4.23 (4.21) | 15.50 (15.59) | 0 (0) | 0 (0) |
| imine-CoTPP-POP | 71.82 (71.07) | 3.56 (3.48) | 13.77 (13.81) | Cl, 1.20 (1.23) | 1.22 (1.23) |
| TPP-PiP(Cl) | 73.51 (73.62) | 4.22(3.95) | 13.56 (13.74) | Cl, 3.86 (3.92) | 0 (0) |
| TPP-PiP(Br) | 66.21 (66.38) | 3.74 (3.57) | 12.24 (12.39) | Br, 2.15 (2.21) | 0 (0) |
| TPP-PiP(I) | 59.85 (60.13) | 3.46 (3.23) | 11.13 (11.22) | I, 1.92 (2.00) | 0 (0) |
| CoTPP-PiP(Cl) | 65.89 (66.13) | 3.54 (3.33) | 12.26 (12.34) | Cl, 3.24 (3.30) | 1.02 (1.10) |
| CoTPP-PiP(Br) | 59.32 (59.16) | 3.37 (3.18) | 10.79 (11.04) | Br, 1.92 (1.96) | 0.93 (0.98) |
| CoTPP-PiP(I) | 55.78 (55.04) | 2.98 (2.77) | 10.98 (10.27) | I, 1.67 (1.83) | 0.87 (0.92) |
| CoTPP-PiP(Br) after 8 cycles | 59.25 | 3.43 | 10.93 | Br, 1.89 | 0.89 |

[a] Theoretical value in the parenthesis.

## 4. Thermogravimetric Analysis

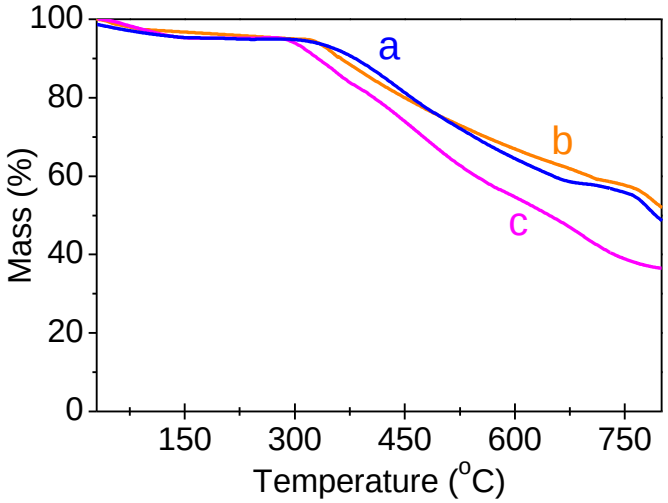


**Figure S1** TGA curves of CoTPP-PiP(Cl) (a), CoTPP-PiP(Br) (b) and CoTPP-PiP(I) (c).

## 5. PXRD Patterns

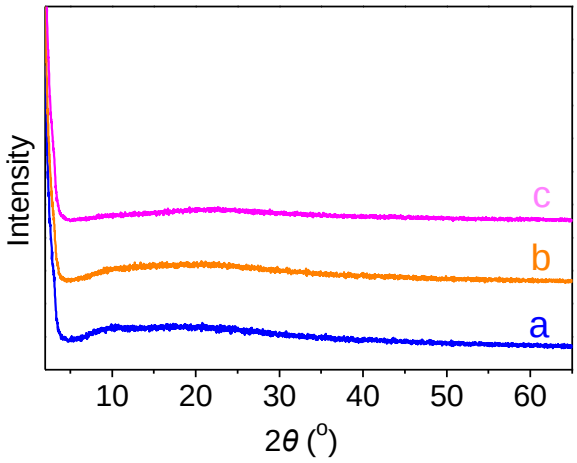


**Figure S2** PXRD curves of CoTPP-PiP(Cl) (a), CoTPP-PiP(Br) (b) and CoTPP-PiP(I) (c).

## 6. $CO_2$ Sorption Isotherms and Selectivity of $CO_2$ over $N_2$

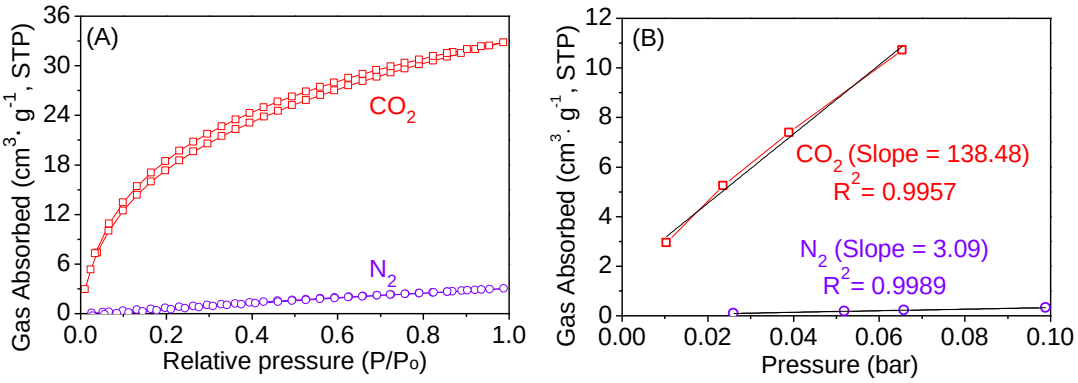


**Figure S3** Gas sorption isotherms (A) and adsorption selectivity of $CO_2$ over $N_2$ for CoTPP-PiP(Br) from initial slope calculations of $CO_2$ and $N_2$ isotherms(B) at 273 K

## 7. Characterization for the Reused Catalyst

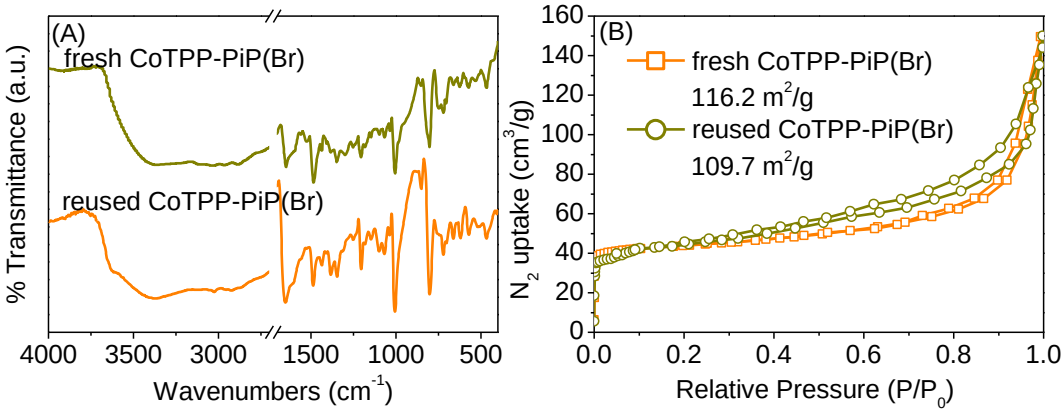


**Figure S4.** FT-IR spectra (A) and $N_2$ sorption isotherms (B) of the fresh and reused CoTPP-PiP(Br)

## 8. Activity Comparison

**Table S2.** Results of the cycloaddition reaction of $CO_2$ with PO over various metal-free catalysts.[a]

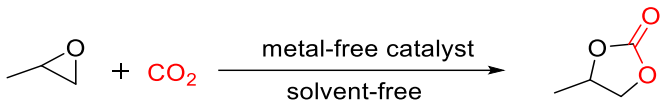


| Entry | Catalyst | $CO_2$ (MPa) | T (°C) | Conv. [b] (%) | Yield [b] (%) |
|---|---|---|---|---|---|
| 1 | blank | 1.0 | 80 | n.d. | n.d |
| 2 | TAPP | 1.0 | 80 | 15 | 14 |
| 3 | imine-TPP-POP | 1.0 | 80 | 9 | 9 |
| 4 | TPP-PiP(Br) | 1.0 | 80 | 98 | 98 |
| 5 | TPP-PiP(Cl) | 1.0 | 80 | 88 | 88 |
| 6 | TPP-PiP(I) | 1.0 | 80 | 56 | 55 |
| 7[c] | TPP-PiP(Br) | 1.0 | 80 | 63 | 63 |
| 8[d] | TPP-PiP(Br) | 0.5 | 80 | 74 | 74 |
| 9 | TPP-PiP(Br) | 1.0 | 60 | 65 | 65 |

[a] Reaction conditions: PO (3.0 mmol), catalyst (0.4 mol%, catalyst amount equal to the amount of ionic liquids), initial $CO_2$ pressure (1.0 MPa), 24 h.

[b] Determined by GC using biphenyl as an internal standard.

[c] Catalyst (0.1 mol%)

[d] Keeping $CO_2$ pressure at 0.5 MPa.

## 9. Activity Comparison

**Table S3**. Activity comparison in the propylene oxide to propylene carbonate conversion reaction

| Catalyst (mol%) | Additive (mol%) | Solvent | T (°C) | $CO_2$ (MPa) | t (h) | Yield (%) | Ref. |
|---|---|---|---|---|---|---|---|
| CoTPP-PiP(Br) | -[a] | - | 80 | 1.0 | 12 | 99 | This work |
| FIP-Im (5) | | | 80 | 1.0 | 10 | 99 | 4 |
| PDBA-Cl-SCD (2.4) | - | - | 90 | 0.1 | 6 | 99.6 | 5 |
| NP-NHC (5 wt%) | - | - | 120 | 0.1 | 24 | 98 | 6 |
| NPILs-BPA (0.5) | - | | 150 | 2.0 | 4 | 98 | 7 |
| SBA-[V0.15OH0.60]$R_2$37 (0.65) | - | | 140 | 2.0 | 6 | 99 | 8 |
| TBB-Bpy-a (80 mg) | - | - | 120 | 1.0 | 4 | 99 | 9 |
| PDMBr (1.3) | - | - | 110 | 1.0 | 4 | 98.7 | 10 |
| TBB-Bpy-a (4 wt%) | - | - | 90 | 1.0 | 12 | 99 | 11 |
| mesoPILC (50 mg) | - | | 150 | 1.0 | 6 | 92 | 12 |
| DVB-HTA (0.22) | - | | 120 | 1.2 | 6 | 93 | 13 |
| SYSU-Zn@IL2 (0.16) | - | - | 80 | 1.0 | 12 | 99 | 14 |
| DVB@ISA (0.25) | - | - | 60 | 1.0 | 24 | 17 | 15 |
| Al-CPOP (1) | - | - | 120 | 0.1 | 24 | 67 | 16 |
| TBB-Bpy@Salen-Co (0.2) | - | - | 60 | 1.0 | 6 | 99.2 | 17 |
| Mg-por/pho@POP (0.5) | - | - | 140 | 3.0 | 1 | 78 | 18 |
| $PPh_3$-ILBr-$ZnBr_2$@POPs (0.0125) | - | - | 120 | 3.0 | 1 | 44 | 19 |
| 1P$^+$Br-&$ZnBr_2$-1$PPh_3$@POPs (0.0125) | - | - | 120 | 3.0 | 1 | 49.8 | 20 |
| Py-Zn@MA (0.28) | - | - | 150 | 2.0 | 6 | 96 | 21 |
| POM3-IM (5) | - | EtOH | 120 | 1.0 | 8 | 96 | 22 |
| HIP-Br-2 (4) | $ZnBr_2$ (4) | DMF | 25 | 0.1 | 96 | 99 | 23 |
| Zn@SBMMP (1.2) | TBAB (1.8) | DCE | 80 | 2.0 | 4 | 95 | 24 |
| g-$C_3N_4$-475-NaOH (0.4 g) | $ZnI_2$ (38 mg) | | 140 | 2.0 | 6 | 89.5 | 25 |
| Bp-Zn@MA (0.086) | TBAB (0.55) | | 100 | 1.0 | 1.5 | 99 | 26 |
| PPS⊂COF-TpBpy-Cu (0.1) | - | | 25 | 0.1 | 72 | 94 | 27 |
| IL-ZIF-90 (0.5) | - | | 120 | 1.0 | 3 | 697 | 28 |
| HF-MOP (5) | TBAI (5) | | 80 | 2.0 | 18 | 89 | 29 |
| Co-CMP | TBAB (7.2) | | 100 | 3.0 | 1 | 98.1 | 30 |
| Al-MON (0.05) | TBAC (0.15) | | 60 | 1.0 | 12 | 71 | 31 |
| In-MOF (0.23) | TBAB (2.5) | | 80 | 2.0 | 4 | 93.9 | 32 |
| Cu-MOF (0.2) | TBAB (10) | | 25 | 0.1 | 48 | 96 | 33 |
| Co/POP-TPP (0.22) | TBAB (0.7) | - | 29 | 0.1 | 24 | 94.8 | 34 |
| Cu/POP-Bpy (0.5) | TBAB (7) | - | 29 | 0.1 | 48 | 99 | 35 |

[a] Not added additive or solvent.

## 10. NMR Spectra

***The $^{1}H$ NMR and $^{13}C$ NMR spectral copies of various synthesized cyclic carbonates:***

***4-methyl-1,3-dioxolan-2-one:***

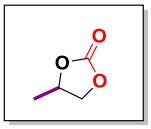

$^{1}H$ NMR ($CDCl_3$, 400 MHz, 25 °C, TMS): δ (ppm) = 4.77-4.86 (m, 1H, ring C*H*-$CH_3$), 4.49-4.53 (t, 1H, *J* = 8 Hz, ring $CH_2$), 1.41-1.43 (d, 3H, *J* = 8 Hz, $CH_3$); $^{13}C$ NMR ($CDCl_3$, 101 MHz, 25 °C, TMS): δ (ppm) = 155.15, 73.70, 70.72, 19.31.

***4-(chloromethyl)-1,3-dioxolan-2-one:***

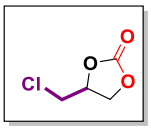

$^{1}H$ NMR ($CDCl_3$, 400 MHz, 25 °C, TMS): δ (ppm) = 4.98-5.04 (m, 1H, C*H*-$CH_2$), 4.59-4.63 (t, *J* = 8 Hz, 1H, ring $CH_2$), 4.40-4.44 (dd, *J* = 8 Hz, 4 Hz, 1H, ring $CH_2$), 3.72-3.84 (m, 2 H, $CH_2$-Cl); $^{13}C$ NMR ($CDCl_3$, 101 MHz, 25 °C, TMS): δ (ppm) = 154.35, 74.38, 67.00, 43.86.

***4-ethyl-1,3-dioxolan-2-one:***

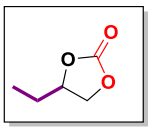

$^{1}H$ NMR ($CDCl_3$, 500 MHz, 25 °C, TMS): δ (ppm) = 4.58-4.63 (m, 1H), 4.45-4.48 (t, *J* = 10 Hz, 1H), 4.00-4.03 (t, *J* = 10 Hz, 1H), 1.64-1.75 (m, 2H), 0.92-0.95 (t, *J* = 10 Hz, 3H); $^{13}C$ NMR ($CDCl_3$, 101 MHz, 25 °C, TMS): δ (ppm) = 155.21, 78.11, 69.06, 26.79, 8.38.

***4-butyl-1,3-dioxolan-2-one:***

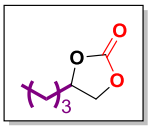

$^{1}H$ NMR ($CDCl_3$, 500 MHz, 25 °C, TMS): δ (ppm) = 4.59-4.64 (m, 1H), 4.42-4.45 (t, *J* = 10 Hz, 1H), 3.95-3.98 (t, *J* = 10 Hz, 1H), 1.63-1.71 (m, 1H), 1.55-1.62 (m, 1H), 1.19-1.36 (m, 4H), 0.79-0.82 (t, *J* = 10 Hz, 3H); $^{13}C$ NMR ($CDCl_3$, 126 MHz, 25 °C, TMS): δ (ppm) = 155.16, 77.15, 69.41, 33.35, 26.33,22.13, 13.66.

***4-hexyl-1,3-dioxolan-2-one:***

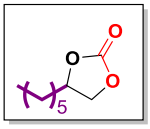

$^{1}H$ NMR ($CDCl_3$, 500 MHz, 25 °C, TMS): δ (ppm) = 4.62-4.68 (m, 1H), 4.46-4.49 (t,

*J* = 10 Hz, 1H), 3.99-4.02 (t, *J* = 10 Hz, 1H), 1.69-1.76 (m, 1H), 1.59-1.65 (m, 1H), 1.34-1.44 (m, 1H), 1.20-1.33 (m, 7H), 0.80-0.83 (t, *J* = 10 Hz, 3H); $^{13}$C NMR ($CDCl_3$, 126 MHz, 25 °C, TMS): δ (ppm) = 155.16, 77.14, 69.42, 33.77, 31.46, 28.73, 24.26, 22.39, 13.92.

***4-((allyloxy)methyl)-1,3-dioxolan-2-one:***

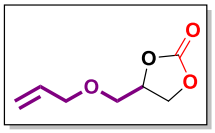

$^{1}$H NMR ($CDCl_3$, 400 MHz, 25 °C, TMS): δ (ppm) = 5.83-5.92 (m, 1H), 5.19-5.31 (dd, *J* = 10 Hz, 2H), 4.84-4.87 (m, 1H), 4.50-4.54 (t, *J* = 8 Hz, 1H), 4.38-4.42 (d, *J* = 8 Hz, 1H), 4.01-4.10 (m, 2H), 3.60-3.73 (m, 2H). $^{13}$C NMR ($CDCl_3$, 101 MHz, 25 °C, TMS): δ (ppm) = 155.06, 133.17, 117.79, 75.17, 72.51, 68.86, 66.27.

***4-phenyl-1,3-dioxolan-2-one:***

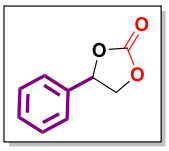

$^{1}$H NMR ($CDCl_3$, 400 MHz, 25 °C, TMS): δ (ppm) = 7.28-7.38 (m, 4H, ring ArH), 5.58-5.62 (t, 1H, *J* = 8 Hz, PhCHO), 4.71-4.75 (t, 1H, *J* = 8 Hz, $OCH_2$), 4.26-4.30 (t, 1H, *J* = 8 Hz, $OCH_2$); $^{13}$C NMR ($CDCl_3$, 101 MHz, 25 °C, TMS): δ (ppm) = 153.75, 134.78, 128.72, 128.23, 124.83, 76.95, 70.13.

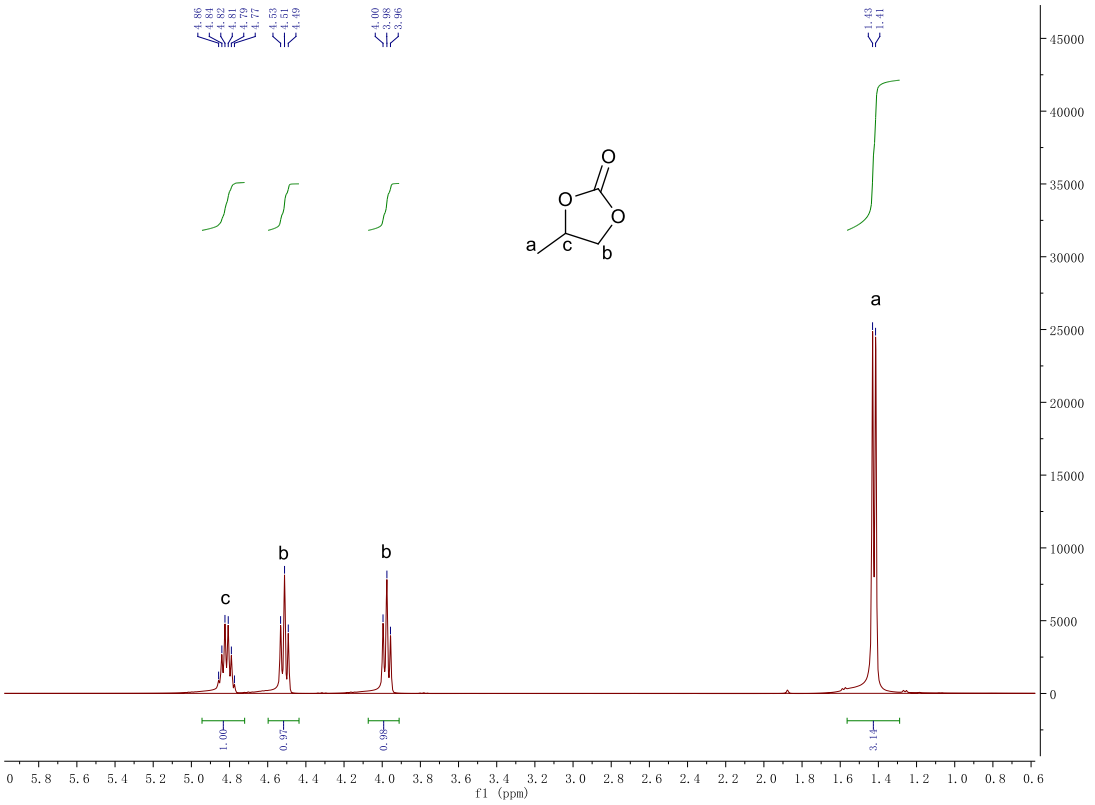
4.86
4.84
4.82
4.81
4.79
4.77
4.53
4.51
4.49
4.00
3.98
3.96
1.43
1.41
O
O
O
a
c
b
a
b
b
c
1.00
0.97
0.98
3.14
f1 (ppm)

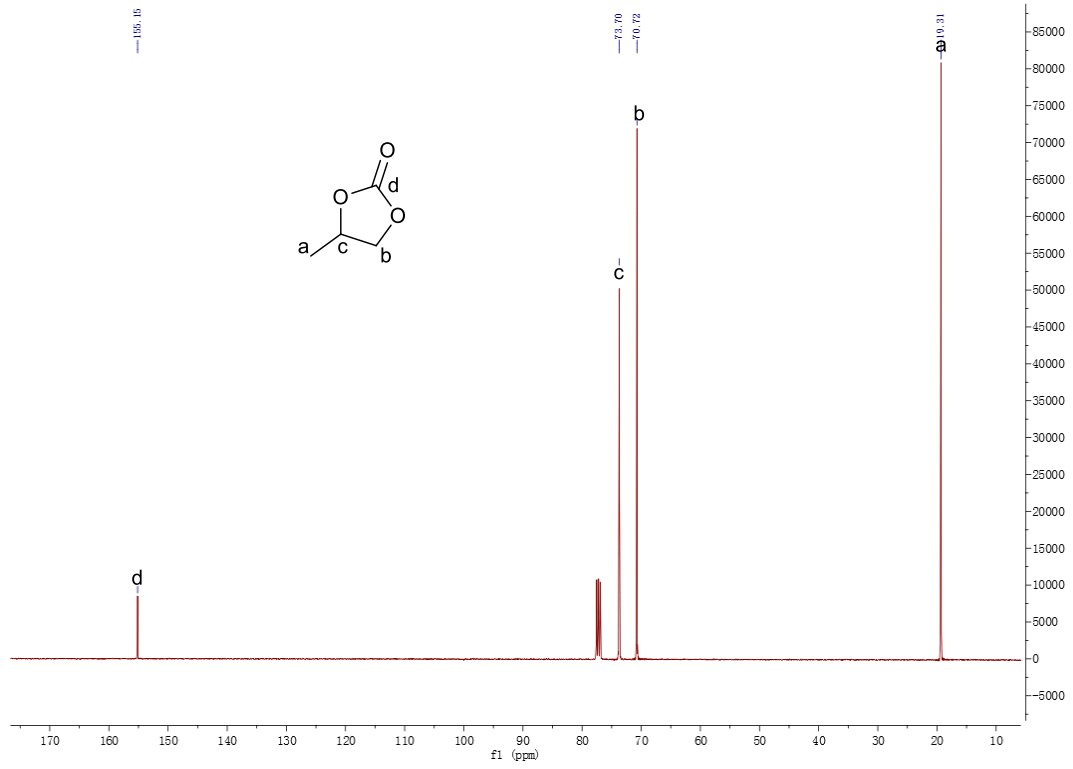
155.15
73.70
70.72
19.31
O
O
O
d
a
c
b
d
c
b
a
f1 (ppm)

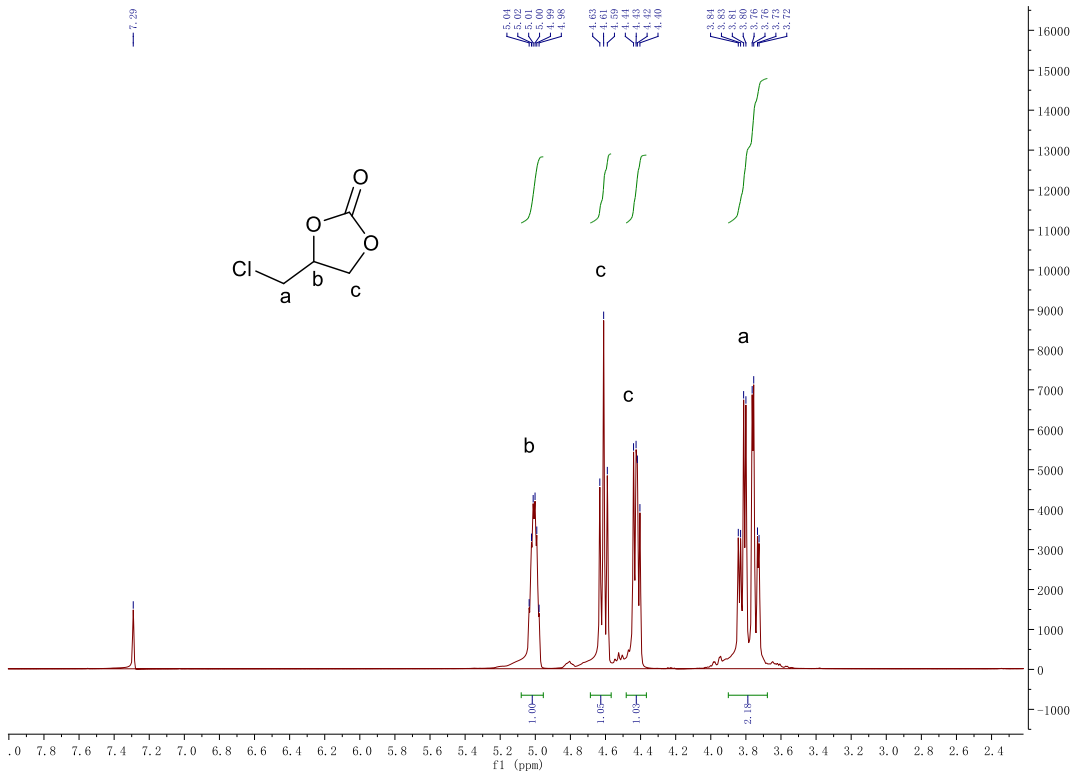
7.29
5.04
5.02
5.01
5.00
4.99
4.98
4.63
4.61
4.59
4.44
4.43
4.42
4.40
3.84
3.83
3.81
3.80
3.75
3.76
3.73
3.72
O
O
O
Cl
a
b
c
c
a
c
b
1.00
1.05
1.03
2.18
f1 (ppm)

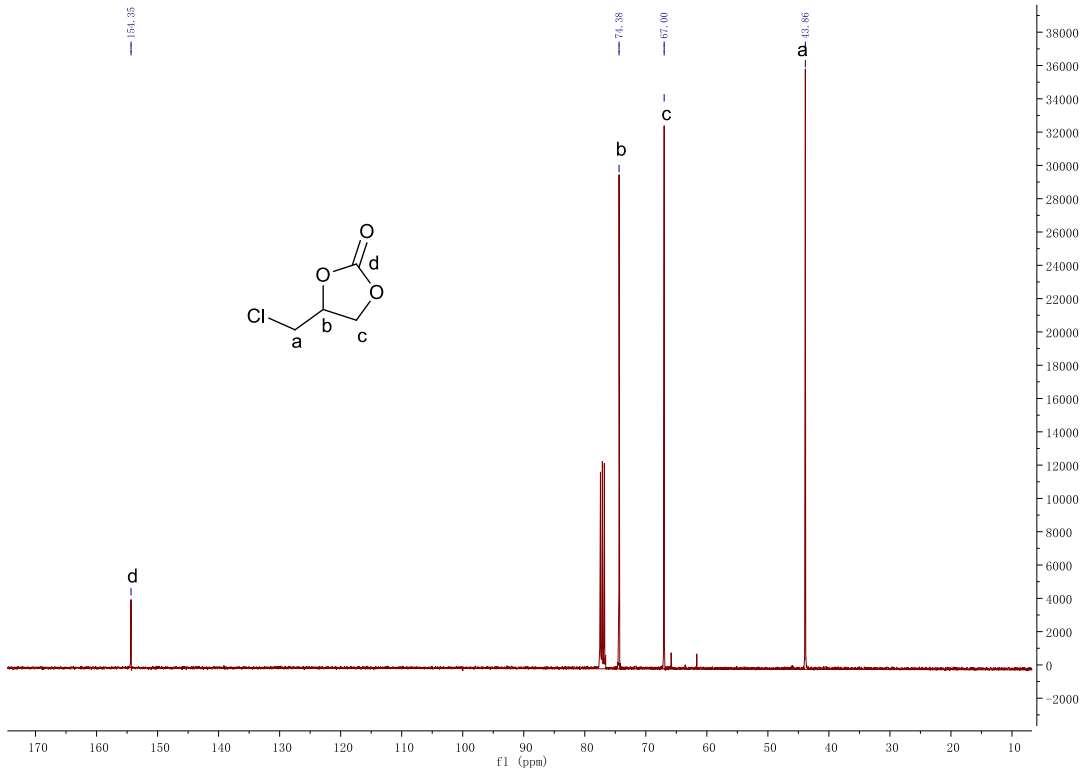
154.35
74.38
67.00
43.86
O
O
d
O
Cl
a
b
c
d
a
c
b
f1 (ppm)

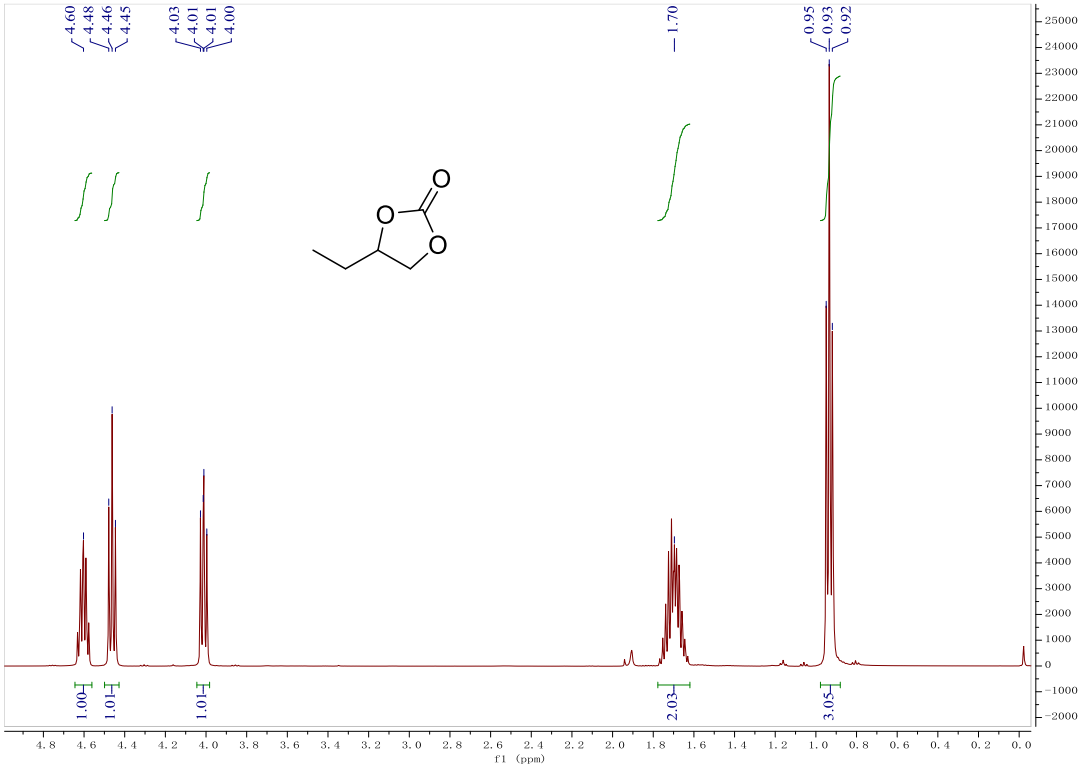
4.60
4.48
4.46
4.45
4.03
4.01
4.01
4.00
1.70
0.95
0.93
0.92
1.00
1.01
1.01
2.03
3.05
f1 (ppm)

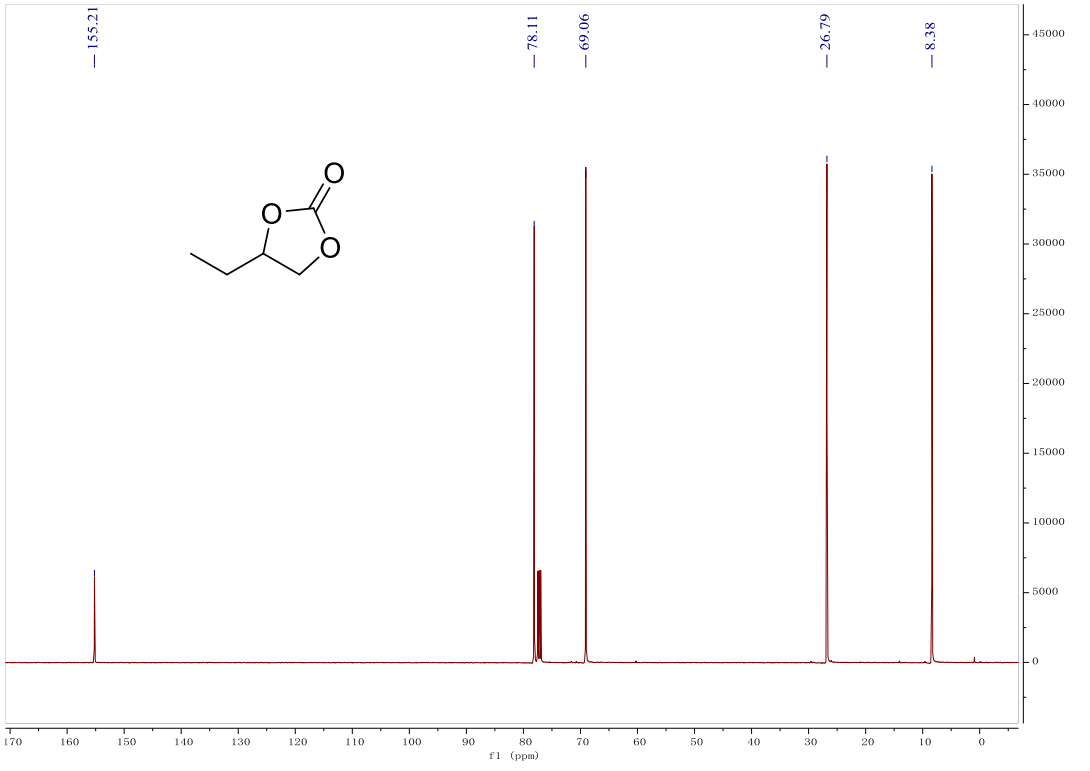
155.21
78.11
69.06
26.79
8.38
f1 (ppm)

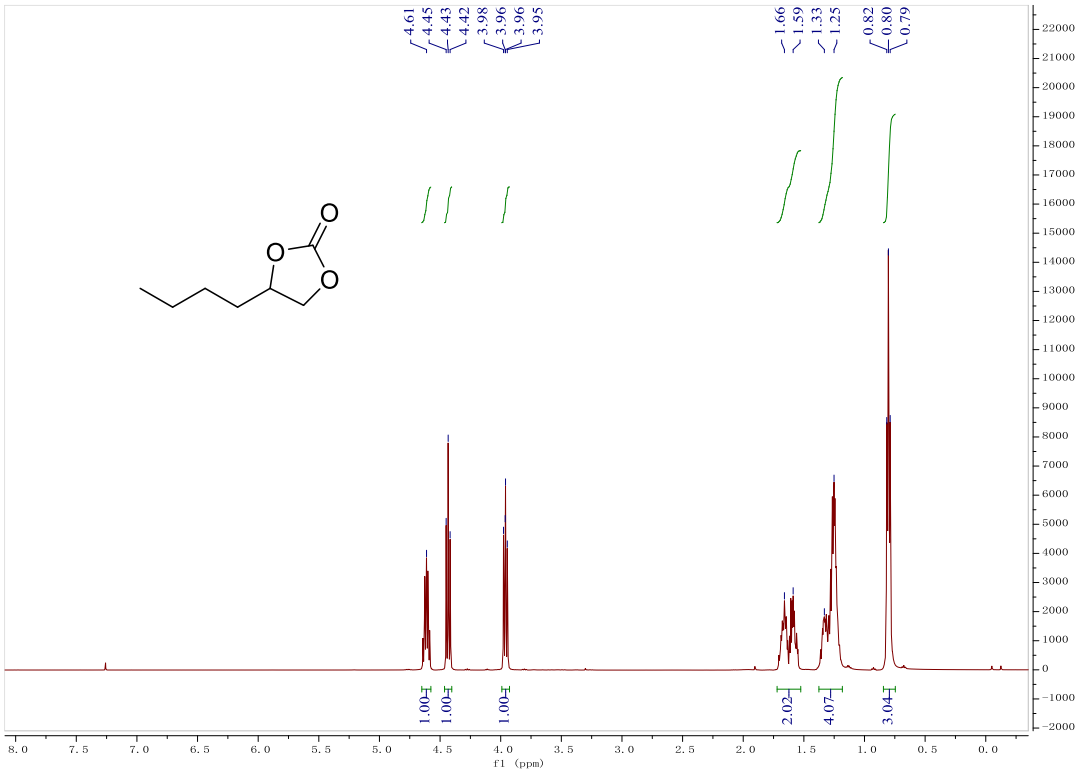
4.61
4.45
4.43
4.42
3.98
3.96
3.96
3.95
1.66
1.59
1.33
1.25
0.82
0.80
0.79
1.00
1.00
1.00
2.02
4.07
3.04
f1 (ppm)

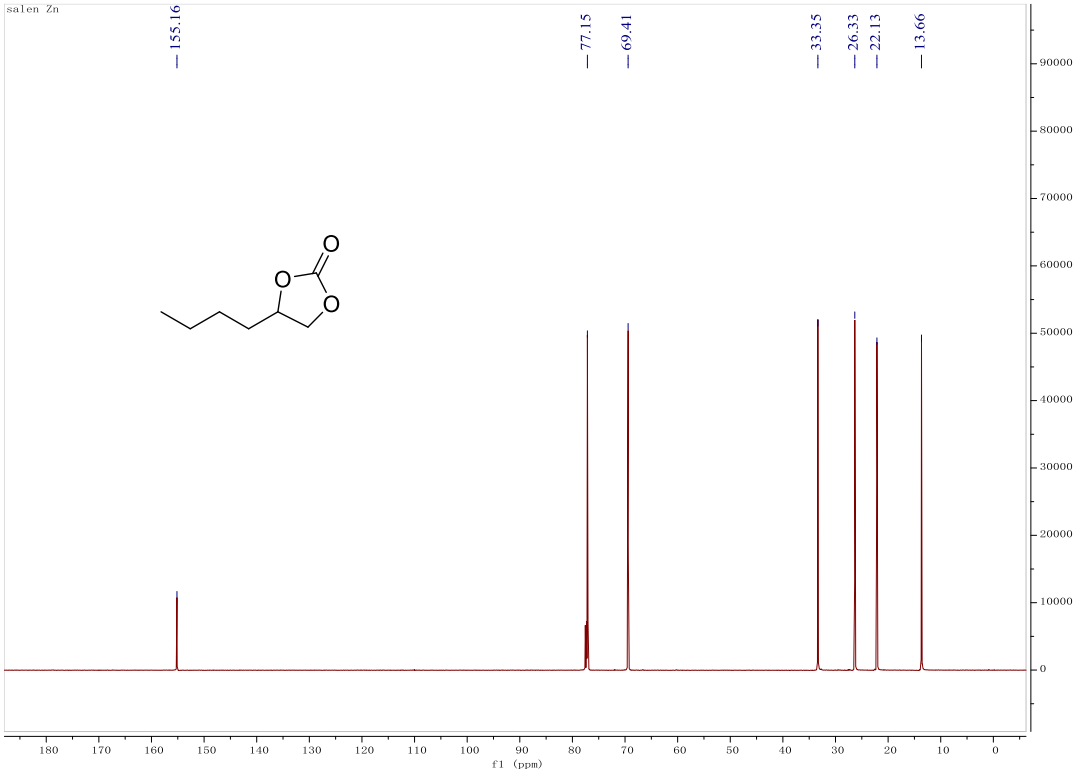
salen Zn
155.16
77.15
69.41
33.35
26.33
22.13
13.66
f1 (ppm)

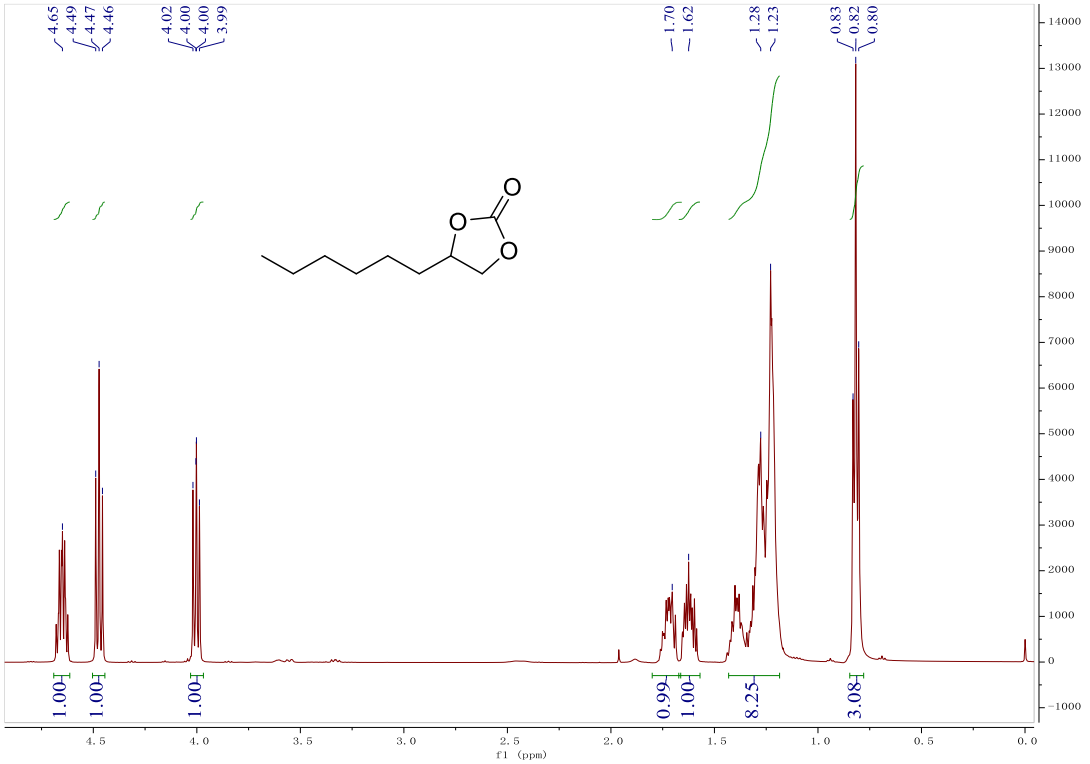
4.65
4.49
4.47
4.46
4.02
4.00
4.00
3.99
1.70
1.62
1.28
1.23
0.83
0.82
0.80
1.00
1.00
1.00
0.99
1.00
8.25
3.08
f1 (ppm)

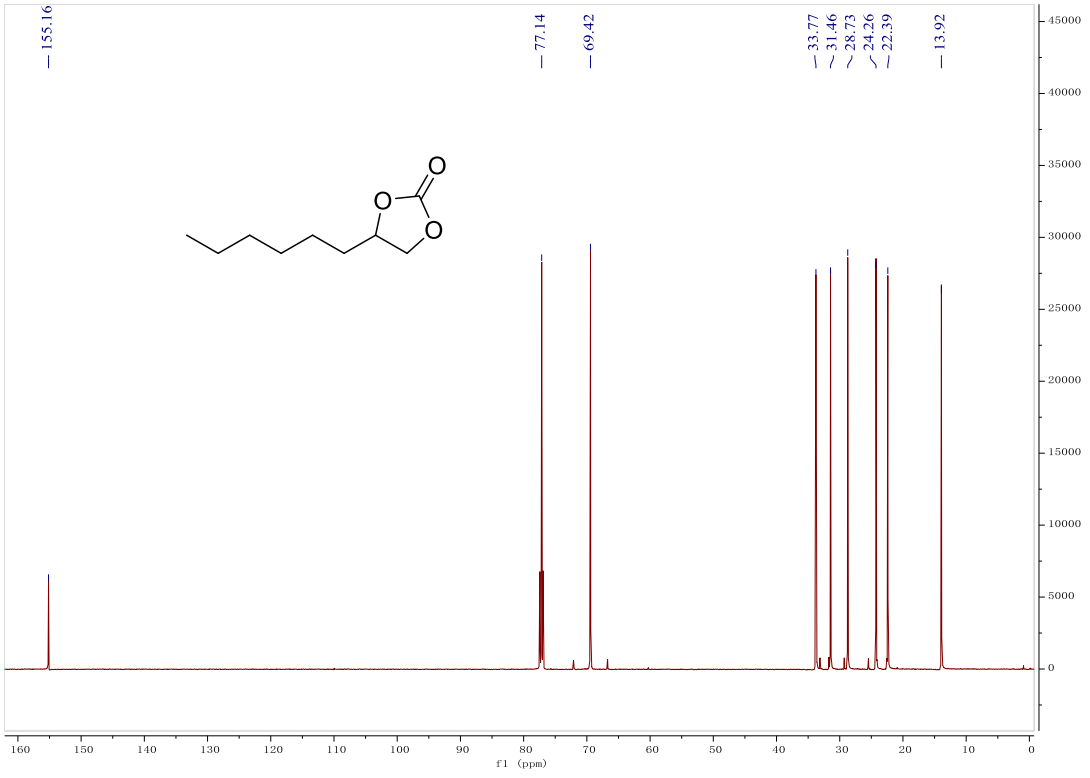
155.16
77.14
69.42
33.77
31.46
28.73
24.26
22.39
13.92
f1 (ppm)

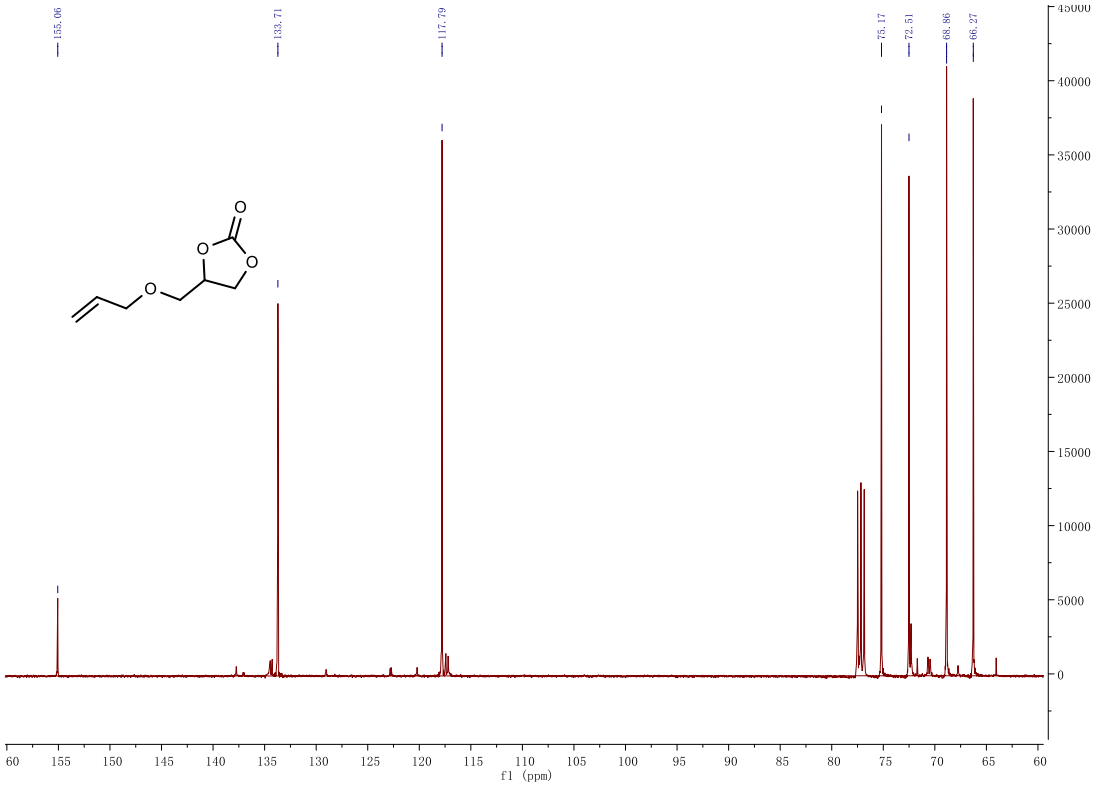
155.06
133.71
117.79
75.17
72.51
68.86
66.27
f1 (ppm)

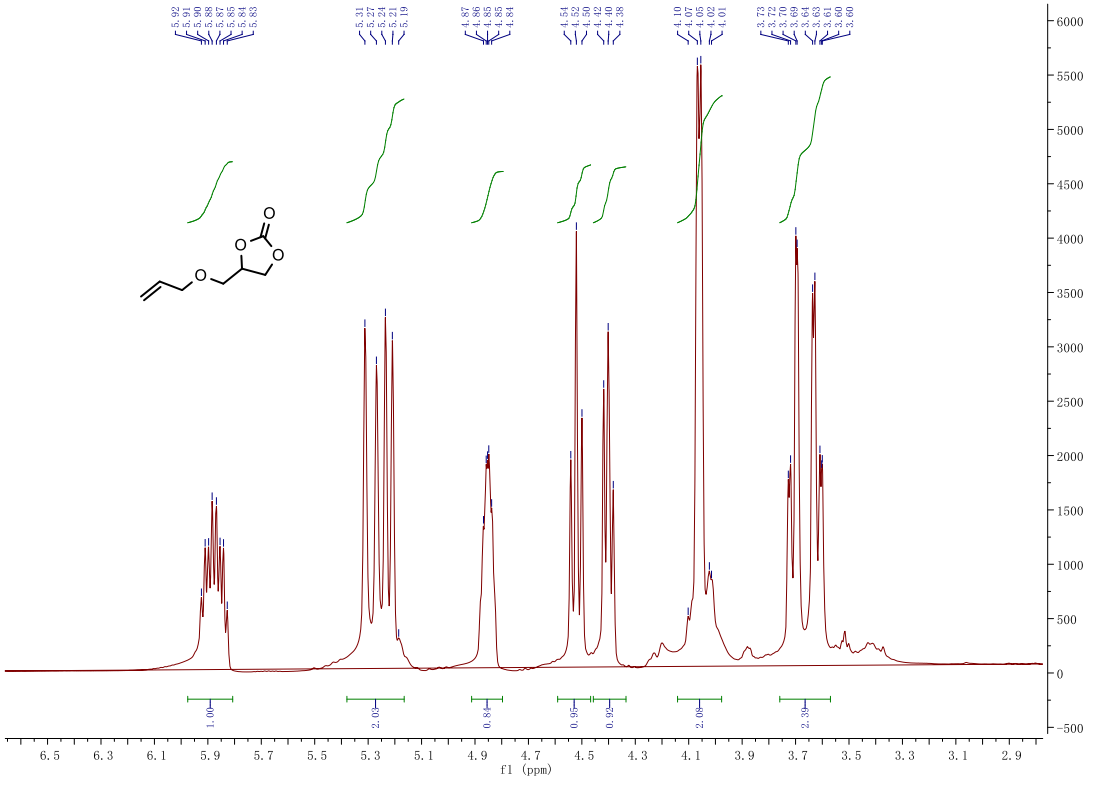
5.92
5.91
5.90
5.88
5.87
5.85
5.84
5.83
5.31
5.27
5.24
5.21
5.19
4.87
4.86
4.85
4.85
4.84
4.54
4.52
4.50
4.42
4.40
4.38
4.10
4.07
4.05
4.02
4.01
3.73
3.72
3.70
3.69
3.64
3.63
3.61
3.60
3.60
1.00
2.03
0.84
0.95
0.92
2.09
2.39
f1 (ppm)

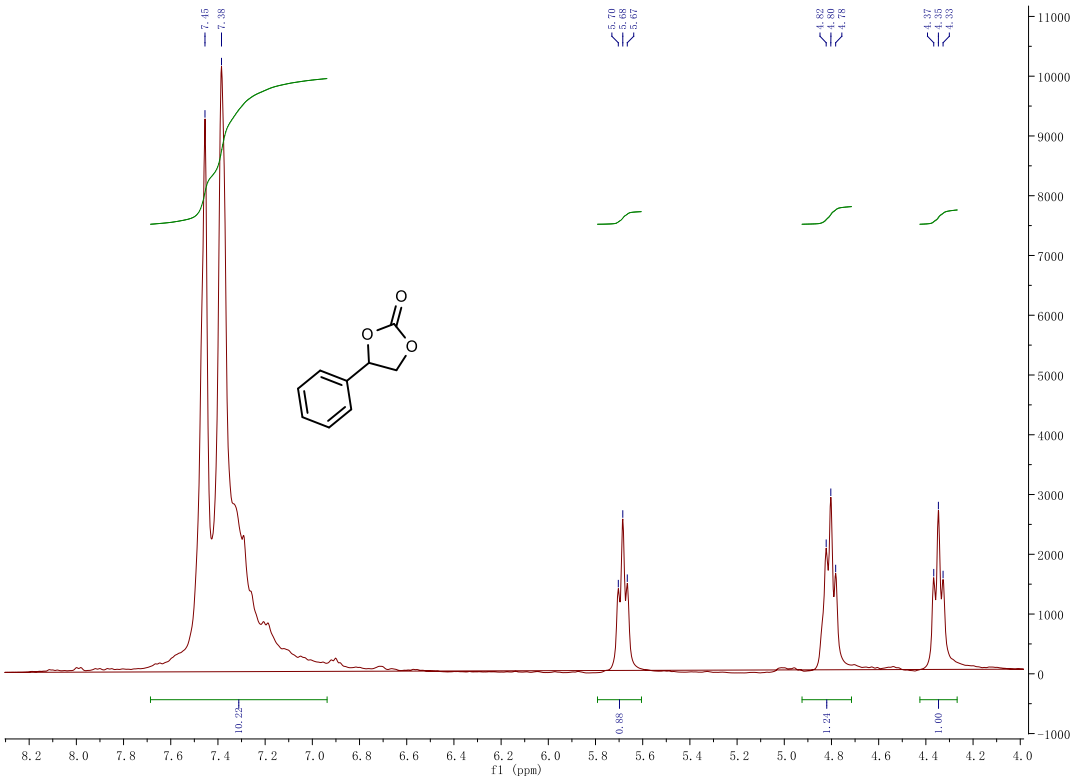
7.45
7.38
5.70
5.68
5.67
4.82
4.80
4.78
4.37
4.35
4.33
10.22
0.88
1.24
1.00
f1 (ppm)

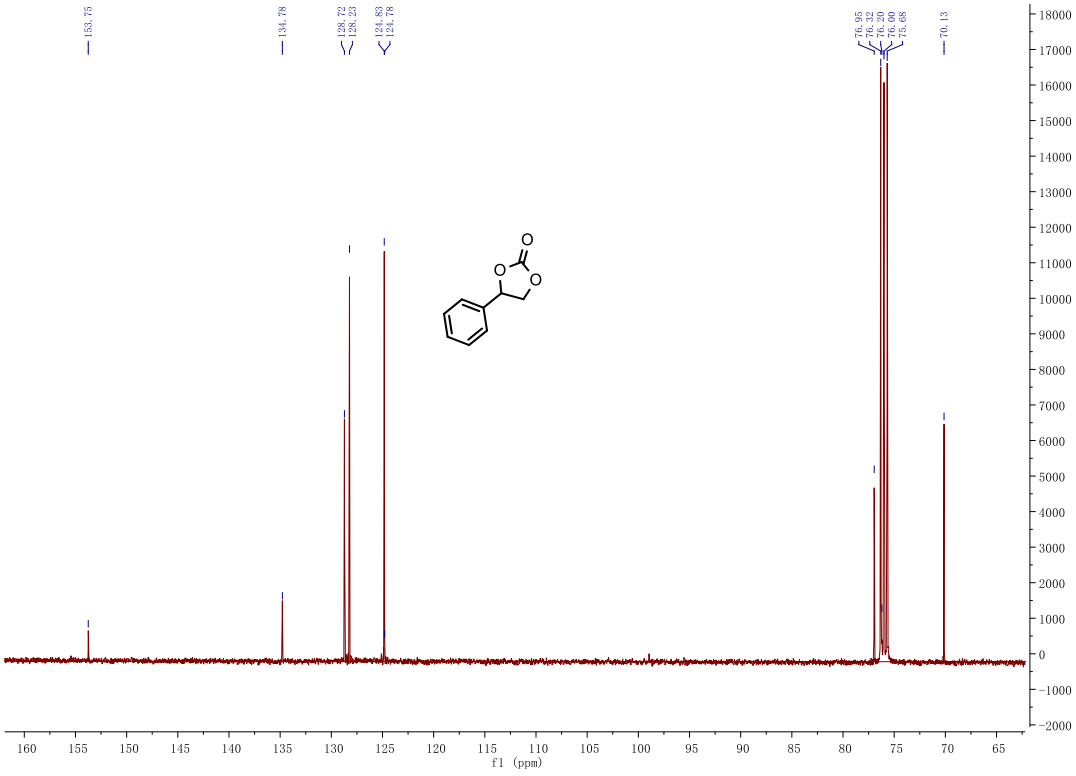
153.75
134.78
128.72
128.23
124.83
124.78
76.95
76.32
76.20
76.00
75.68
70.13
f1 (ppm)

## References


(1) Bettelheim, A.; White, B. A.; Raybuck, S. A.; Murray, R. W. Electrochemical polymerization of amino-, pyrrole-, and hydroxy-substituted tetraphenylporphyrins. *Inorg. Chem.* **1987,** *26*, 1009-1017.

(2) Xu, X. L.; Lin, F. W.; Xu, W.; Wu, J.; Xu, Z. K. Highly sensitive INHIBIT and XOR logic gates based on ICT and ACQ emission switching of a porphyrin derivative. *Chem. Eur. J.* **2015,** *21*, 984-987.

(3) Lin, S.; Diercks, C. S.; Zhang, Y.-B.; Kornienko, N.; Nichols, E. M.; Zhao, Y.; Paris, A. R.; Kim, D.; Yang, P.; Yaghi, O. M.; Chang, C. J. Covalent organic frameworks comprising cobalt porphyrins for catalytic $CO_2$ reduction in water. *Science* **2015,** *349*, 1208-1213.

(4) Chen, Y.; Luo, R.; Bao, J.; Xu, Q.; Jiang, J. u.; Zhou, X.; Ji, H. Function-oriented ionic polymers having high-density active sites for sustainable carbon dioxide conversion. *J. Mater. Chem. A* **2018,** *6*, 9172-9182.

(5) Xie, Y.; Sun, Q.; Fu, Y.; Song, L.; Liang, J.; Xu, X.; Wang, H.; Li, J.; Tu, S.; Lu, X.; Li, J. Sponge-like quaternary ammonium-based poly(ionic liquid)s for high $CO_2$ capture and efficient cycloaddition under mild conditions. *J. Mater. Chem. A* **2017,** *5*, 25594-25600

(6) Talapaneni, S. N.; Buyukcakir, O.; Je, S. H.; Srinivasan, S.; Seo, Y.; Polychronopoulou, K.; Coskun, A. Nanoporous polymers incorporating sterically confined N-heterocyclic carbenes for simultaneous $CO_2$ capture and xconversion at ambient pressure. *Chem. Mater.* **2015,** *27*, 6818-6826.

(7) Liu, Y.; Cheng, W.; Zhang, Y.; Sun, J.; Zhang, S. Controllable preparation of phosphonium-based polymeric ionic liquids as highly selective nanocatalysts for the chemical conversion of $CO_2$ with epoxides. *Green Chem.* **2017,** *19*.

(8) Jayakumar, S.; Li, H.; Zhao, Y.; Chen, J.; Yang, Q. Cocatalyst-free hybrid ionic liquid (IL)-based porous materials for efficient synthesis of cyclic carbonates through a cooperative activation pathway. *Chem. Asian J.* **2017,** *12*, 577-585.

(9) Leng, Y.; Lu, D.; Jiang, P.; Zhang, C.; Zhao, J.; Zhang, W. Highly cross-linked cationic polymer microspheres as an efficient catalyst for facile $CO_2$ fixation. *Catal. Commun.* **2016,** *74*, 99-103.

(10) Wang, X.; Zhou, Y.; Guo, Z.; Chen, G.; Li, J.; Shi, Y.; Liu, Y.; Wang, J. Heterogeneous conversion of $CO_2$ into cyclic carbonates at ambient pressure catalyzed by ionothermal-derived meso-macroporous hierarchical poly(ionic liquid)s. *Chem. Sci.* **2015,** *6*, 6916-6924.

(11) Buyukcakir, O.; Je, S. H.; Talapaneni, S. N.; Kim, D.; Coskun, A. Charged covalent triazine frameworks for $CO_2$ capture and conversion. *ACS Appl. Mater. Interfaces* **2017,** *9*, 7209-7216.

(12) Soll, S.; Zhang, P.; Zhao, Q.; Wang, Y.; Yuan, J. Mesoporous zwitterionic poly(ionic liquid)s: intrinsic complexation and efficient catalytic fixation of CO2. *Polym. Chem.* **2013,** *4*, 5048-5051.

(13) Cai, S.; Zhu, D.; Zou, Y.; Zhao, J. Porous polymers bearing functional quaternary ammonium salts as efficient solid catalysts for the fixation of $CO_2$ into cyclic carbonates. *Nanoscale Res. Lett.* **2016,** *11*, 1-9.

(14) Chen, Y.; Luo, R.; Xu, Q.; Jiang, J.; Zhou, X.; Ji, H. Metalloporphyrin polymers with intercalated ionic liquids for synergistic $CO_2$ fixation via cyclic carbonate production. *ACS Sustainable Chem. Eng.* **2018,** *6*, 1074-1082.

(15) Luo, R.; Chen, Y.; He, Q.; Lin, X.; Xu, Q.; He, X.; Zhang, W.; Zhou, X.; Ji, H. Metallosalen-based ionic porous polymers as bifunctional catalysts for the conversion of $CO_2$ into

valuable chemicals. *ChemSusChem* **2017,** *10*, 1526-1533.
(16) Liu, T.-T.; Liang, J.; Huang, Y.-B.; Cao, R. A bifunctional cationic porous organic polymer based on a Salen-(Al) metalloligand for the cycloaddition of carbon dioxide to produce cyclic carbonates. *Chem. Commun.* **2016,** *52*, 13288-13291.
(17) Leng, Y.; Lu, D.; Zhang, C.; Jiang, P.; Zhang, W.; Wang, J. Ionic polymer microspheres bearing a $Co^{III}$-salen moiety as a bifunctional heterogeneous catalyst for the efficient cycloaddition of $CO_2$ and epoxides. *Chem. Eur. J.* **2016,** *22*, 8368-8375.
(18) Wang, W.; Wang, Y.; Li, C.; Yan, L.; Jiang, M.; Ding, Y. State-of-the-art multifunctional heterogeneous POP catalyst for cooperative transformation of $CO_2$ to cyclic carbonates. *ACS Sustainable Chem. Eng.* **2017,** *5*, 4523-4528.
(19) Wang, W.; Li, C.; Yan, L.; Wang, Y.; Jiang, M.; Ding, Y. Ionic liquid/Zn-$PPh_3$ integrated porous organic polymers featuring multifunctional sites: highly active heterogeneous catalyst for cooperative conversion of $CO_2$ to cyclic carbonates. *ACS Catal.* **2016,** *6*, 6091-6100.
(20) Li, C.; Wang, W.; Yan, L.; Wang, Y.; Jiang, M.; Ding, Y. Phosphonium salt and $ZnX_2$–$PPh_3$ integrated hierarchical POPs: tailorable synthesis and highly efficient cooperative catalysis in $CO_2$ utilization. *J. Mater. Chem. A* **2016,** *4*, 16017-16027.
(21) Li, H.; Li, C. Z.; Chen, J.; Liu, L. N.; Yang, Q. H. Synthesis of pyridine-zinc-based porous organic polymer for cocatalyst-free cycloaddition of epoxides. *Chem. Asian J.* **2017,** *12*, 1095–1103
(22) Wang, J.; Sng, W.; Yi, G.; Zhang, Y. Imidazolium salt-modified porous hypercrosslinked polymers for synergistic $CO_2$ capture and conversion. *Chem. Commun.* **2015,** *51*, 12076-12079.
(23) Li, J.; Jia, D.; Guo, Z.; Liu, Y.; Lu, Y.; Zhou, Y.; Wang, J. Imidazolinium based porous hypercrosslinked ionic polymers for efficient $CO_2$ capture and fixation with epoxides. *Green Chem.* **2017,** *19*, 2675-2686.
(24) Bhunia, S.; Molla, R. A.; Kumari, V.; Islam, S. M.; Bhaumik, A. Zn(ii) assisted synthesis of porous salen as an efficient heterogeneous scaffold for capture and conversion of $CO_2$. *Chem. Commun.* **2015,** *51*, 15732-15735.
(25) Xu, J.; Shang, J.-K.; Jiang, Q.; Wang, Y.; Li, Y.-X. Facile alkali-assisted synthesis of g-C3N4materials and their high-performance catalytic application in solvent-free cycloaddition of CO2to epoxides. *RSC Adv.* **2016,** *6*, 55382-55392.
(26) Chen, J.; Li, H.; Zhong, M.; Qihua, Y. Hierarchical mesoporous organic polymer with intercalated metal complex for efficient synthesis of cyclic carbonates from flue gas. *Green Chem.* **2016,** *18*, 6493-6500.
(27) Sun, Q.; Aguila, B.; Perman, J.; Nguyen, N.; Ma, S. Flexibility matters: cooperative active sites in covalent organic framework and threaded ionic polymer. *J. Am. Chem. Soc.* **2016,** *138*, 5790–15796.
(28) Tharun, J.; Bhin, K.-M.; Roshan, R.; Kim, D. W.; Kathalikkattil, A. C.; Babu, R.; Ahn, H. Y.; Won, Y. S.; Park, D.-W. Ionic liquid tethered post functionalized ZIF-90 framework for the cycloaddition of propylene oxide and CO2. *Green Chem.* **2016,** *18*, 2479-2487.
(29) Zhang, X.; Lv, Y.-Z.; Liu, X.-L.; Du, G.-J.; Yan, S.-H.; Liu, J.; Zhao, Z. A hydroxyl-functionalized microporous organic polymer for capture and catalytic conversion of $CO_2$. *RSC Adv.* **2016,** *6*, 76957-76963.
(30) Xie, Y.; Wang, T.-T.; Liu, X.-H.; Zou, K.; Deng, W.-Q. Capture and conversion of $CO_2$ at ambient conditions by a conjugated microporous polymer. *Nat. Commun.* **2013,** *4*, 1960-1966.

(31) Chun, J.; Kang, S.; Kang, N.; Lee, S. M.; Kim, H. J.; Son, S. U. Microporous organic networks bearing metal-salen species for mild $CO_2$ fixation to cyclic carbonates. *J. Mater. Chem. A* **2013,** *1*, 5517-5523.
(32) Liu, L.; Wang, S. M.; Han, Z. B.; Ding, M. L.; Yuan, D. Q.; Jiang, H. L. Exceptionally Robust In-Based Metal-Organic Framework for Highly Efficient Carbon Dioxide Capture and Conversion. *Inorg. Chem.* **2016,** *55*, 3558-3565.
(33) Li, P. Z.; Wang, X. J.; Liu, J.; Lim, J. S.; Zou, R. Q.; Zhao, Y. L. A Triazole-Containing Metal-Organic Framework as a Highly Effective and Substrate Size-Dependent Catalyst for CO2 Conversion. *J. Am. Chem. Soc.* **2016,** *138*, 2142-2145.
(34) Dai, Z.; Sun, Q.; Liu, X.; Bian, C.; Wu, Q.; Pan, S.; Wang, L.; Meng, X.; Deng, F.; Xiao, F.-S. Metalated porous porphyrin polymers as efficient heterogeneous catalysts for cycloaddition of epoxides with $CO_2$ under ambient conditions. *J. Catal.* **2016,** *338*, 202-209.
(35) Dai, Z.; Sun, Q.; Liu, X.; Guo, L.; Li, J.; Pan, S.; Bian, C.; Wang, L.; Hu, X.; Meng, X.; Zhao, L.; Deng, F.; Xiao, F.-S. A hierarchical bipyridine-constructed framework for highly efficient $CO_2$ capture and catalytic conversion. *ChemSusChem* **2017,** *10*, 1186–1192.